MORTAR FINITE VOLUME ELEMENT APPROXIMATIONS OF SECOND ORDER ELLIPTIC PROBLEMS

RICHARD EWING, RAYTCHO LAZAROV, TAO LIN, AND YANPING LIN

ABSTRACT. Application of domain decomposition methods for solvingcomplex problems on parallel computers may lead to a situation when the subdomains are meshed independently and the obtained grids do not match at the subdomain interfaces. In this article we consider mortar finite volume element approximations of second order elliptic equations on nonmatching grids. This means that the discretization of the problem is based on Petrov-Galerkin method with a solution space of continuous over each subdomain piece-wise linear functions and a test space of piece-wise constant functions. We construct and study several mortar spaces that are used in imposing the weak continuity of the discrete solution along the grid interfaces and prove an optimal order convegence in energy norm.

1. INTRODUCTION

With rapidly growing computational capabilities, the finite element analysis has been used in increasingly complicated domains and for solving interacting processes. Often such analysis is accomplished by interaction of several research teams, each coming with its own computer environment and numerical technology. Thus, several aspects of such interaction become crucial for the success of the computations: (1) different processes described by different mathematical problems are interact through the interface coupling conditions; (2) different discretization methods are used in different parts of the domain; (3) each subdomain is gridded independedently of the rest of the domain. For example, one may study fluid/solid stucture interaction or may want to combine finite elements and spectral methods, finite elements and boundary elements, or finite collocation methods with finite differences.

This paper discusses numerical technique which can fall into the third category. Namely, we discuss a numerical method when the domain is split initially into subdomains and then each domain is meshed independently of the others. In general, the meshes do not match at the interfaces and the finite volume element method will lead to nonconforming approximations. The interdomain continuity is enforced only in a weak sense, namely with the help of auxiliary spaces existing at the interfaces. There is a large variety of approaches

Date: February 14, 2000.

1991 *Mathematics Subject Classification.* 76S05, 45K05, 65M12, 65M60, 65R20.

Key words and phrases. mortar element, finite volume, convergence, domain decomposition, non-matching grids, non-overlapping and overlapping domains.

The research of the first and second authors has been partially supported by NSF Grants DMS–9626179, DMS–9706985, DMS–9707930, NCR9710337, DMS-9972147, INT-9901498; EPA Grant R 825207–01–1; two generous awards from Mobil Research and Development; and Texas Higher Education Coordinating Board Advanced Research and Technology Program Grants 010366-168 and 010366-0336. The third author has been supported in part also by the National Science Foundation. The fourth author has been supported in part by the National Science and Energy Research Council. The third and fourth authors thank the Institute for Scientific Computation and the Department of Mathematics at Texas A&M University for the financial support and hospitality during their sabbatical leave from Virginia Tech and the University of Alberta, respectively.

of how to impose this weak continuity. In the mortar finite element method, the jumps between the solutions u_i and u_j defined in the subdomains Ω_i and Ω_j, respectively, at the interface $\Gamma_{ij} = \Omega_i \cap \Omega_j$ is made orthogonal to the mortar space of piecewise polynomials. This so-called two-field method (the field of the solution and the field of the mortars) has a variety of settings and can be found in [6, 8, 10, 17, 27] and the references therein. Another formulation, the so-called three-field method, is based on the attempt to make the jumps $u_j - u$ and $u_i - u$ orthogonal to two separate Lagrange multiplier spaces, with the trace of u introduced as a separate field. This method has even greater flexibility and has been proposed in [2, 12].

Since the introduction of the *mortar method* as a coupling technique between the spectral and finite element methods (see, e.g. [9, 10, 11]), it has become the most important technique in domain decomposition methods for non-matching grids. The active research in this field is motivated by its flexibility and great potential for large-scale parallel computation (see, e.g. [1, 7, 9, 10]). The non-conforming finite element mortar method has been studied in [10], where optimal order convergence in H^1-norm was demonstrated. Three-dimensional mortar finite element analysis has been given in [8] and the $h-p$ version is studied in [28]. Non-mortar mixed finite element approximations for second-order elliptic problems have been discussed in [4].

In recent years, there has been growing interest in the finite volume method (called also control-volume method or box-schemes). This interest is mostly due to the desire to have discretizations which are locally conservative. This is a discrete variant of the property of the continuous model which expresses conservation of a certain quantity (mass, heat, momentum, etc). In the early stages, such methods were based on finite differences on rectangular meshes with quite complicated treatment of the coefficients and the right-hand side (see, for example the classic book [24] and the references therein). Recently, the finite volume approach has been combined with the technique of the finite element method in a new development which is capable of producing accurate approximations on general triangular and quadrilateral grids (see, e.g. [15, 16, 20, 21, 22]). The main advantages of the method are compactness of the discretization stencil, good accuracy, and discrete local mass conservation, which for many applications is the most desirable feature of the approximation.

To the authors' best knowledge, there has not been a study for the mortar finite volume element method. For the reasons outlined above, the mortar finite volume element method is a very attractive solution technique in porous media flow simulations because it combines the flexibility of the finite elment method with the local conservation properties of the finite difference method. This can be considered as an alternative of the mixed method which is very popular in the flow calculations. However, the finite volume element method generates definite problems, while the mixed method produces indefinite algebraic systems.

In this paper, we extend the mortar technique to the finite volume method in two ways. First, following the traditional mortar approach, we use finite volume element approximations only on the subdomains and finite element on the interfaces for Lagrange multipliers. Second, we propose numerical schemes using finite volume element on both the subdomains and on the interfaces. It has been shown on various numerical examples that the latter scheme converges much faster (5-8 times) than the former. For both schemes we obtain an optimal H^1-error estimate assuming that the solution u is $H^{1+\tau_k}(\Omega_k)$-regular for each Ω_k with $0 < \tau_k \leq 1$, where Ω is partitioned into K non-overlapping subdomains Ω_k, $k = 1, \ldots, K$.

This paper is organized as follows. In Subsection 2.1 we state the model problem of second-order elliptic equations and give all necessary notations. The discretization uses triangulations of each subdomain independently of the others. To make the presentation more transparent, in Subsection 2.2 we introduce the mortar finite element approximation of the problem on triangular meshes which are conforming on each subdomain, but are non-confroming across the interdomain boundaries. Next, in Subsection 2.3 we introduce the mortar finite volume element approximation and discuss the properties of the method.

Section 3 contains the main theoretical results of the paper, an optimal H^1-error estimate for the solution u. The proof essentially follows the main ideas and tools in the analysis of the mortar finite elmenent approximations from [6, 8, 9, 10]).

In Section 4 we give sevaral extensions of the mortar finite volume element method. The most interesting one, given in Subsection 4.1, is the method with piecewise constant mortar spaces. This approximation is locally conservative in the whole domain including the finite volumes near the subdomain interfaces. Our computational experiments show that this method is even more accurate than the one proposed in Section 2. Next, in Subsection 4.2 we present extensions of the method to combine finite element and finite volume element approximations and to approximations on triangular and recrangular grids.

A substantial and important part of our paper describes the numerical experiments presented in Section 5. The aim of the experiments is to (1) study the accuracy of the proposed schemes on series of test problems and (2) to study the efficiency of the iterative methods for solving the corresponding system of linear equations.

The preliminary results of this paper were announced in [19].

2. Mortar finite volume elements with non-overlapping domains

2.1. Problem formulation and notations. In this paper we consider the following model second-order elliptic boundary value problem: find $u = u(x) \in H_0^1(\Omega)$ such that

$$\int_\Omega A\nabla u \cdot \nabla v dx = \int_\Omega f v dx \equiv (f, v), \quad \text{for all } v \in H_0^1(\Omega), \tag{2.1}$$

where Ω is a bounded convex polygon in $\mathcal{R}^2$ with a boundary $\partial\Omega$, $A = \{a_{i,j}(x)\}$ is a 2×2 symmetric and uniformly in Ω positive definite matrix, and $f = f(x)$ is a known function in $L^2(\Omega)$. We assume that the coefficients $a_{i,j}(x)$ are piecewise smooth functions having finite jumps at certain lines, so that problem (2.1) has a unique solution in a certain Sobolev space.

Remark 2.1. *One may consider also Neumann and Robin boundary conditions on the whole or on a part of the boundary $\partial\Omega$. The construction of the finite volume approximation and its analysis can be carried out with no additional difficulties. In fact, the finite volume element method was introduced by Baliga and Patankar in* [5] *as an attempt to approximate the flux boundary conditions by finite differences in a consistent and systematic way.*

In order to introduce the mortar approximation, we shall present some standard notation in the domain decomposition method (see, e.g. [6, 7, 8, 9]). We partition the initial domain Ω into K non-overlapping subdomains $\{\Omega_k\}_{1 \leq k \leq K}$, which are assumed to be polygons and arranged in such way that the intersection of two subdomains $\overline{\Omega}_l \cap \overline{\Omega}_k$ as well as the intersection $\partial\Omega \cap \partial\Omega_k$ is either empty, reduced to a vertex or reduced to a common edge. If two subdomains Ω_k and Ω_l are adjacent, Γ_{kl} is the common interface and $\mathbf{n}_{kl}$ is the unit normal from Ω_k to Ω_l and we set $\mathbf{n}_{lk} = -\mathbf{n}_{kl}$. The index kl has no meaning if Ω_k and Ω_l have no common edge. For any k, let $H^1_*(\Omega_k)$ denote the spaces $H^1(\Omega_k)$ if $\text{meas}(\partial\Omega_k \cap \partial\Omega) = 0$, otherwise it coincides with the subspace of $H^1(\Omega_k)$ involving all functions whose trace on the set $\partial\Omega_k \cap \partial\Omega$ is zero, i.e.

$$H^1_*(\Omega_k) = \left\{ v_k \in H^1(\Omega_k) \text{ and } \quad v_k|_{\partial\Omega_k \cap \partial\Omega} = 0, \text{ if } \text{meas}(\partial\Omega_k \cap \partial\Omega) \neq 0 \right\}.$$

Next, we introduce the space

$$\mathcal{X} = \left\{ v \in L^2(\Omega) : \quad v_k = v|_{\Omega_k} \in H^1_*(\Omega_k) \right\} = \prod_{k=1}^{K} H^1_*(\Omega_k)$$

equipped with the semi-norm and norm:

$$|v|^2_{\mathcal{X}} = \sum_{k=1}^{K} |v_k|^2_{H^1(\Omega_k)}, \quad ||v||^2_{\mathcal{X}} = |v|^2_{\mathcal{X}} + \sum_{k=1}^{K} ||v_k||^2_{L^2(\Omega_k)},$$

where $|v_k|_{H^1(\Omega_k)}$ denotes the semi-norm in $H^1(\Omega_k)$. We shall also use the notation

$$H_0(\text{div}, \Omega) = \{ q \in H(\text{div}, \Omega) : \quad \mathbf{q} \cdot \mathbf{n}|_{\partial\Omega} = 0 \},$$

where $H(\text{div}, \Omega)$ is the space of all vector-functions in $(L^2(\Omega))^2$ whose divergence is in $L^2(\Omega)$, $\mathbf{n}$ is the unit outward normal vector to $\partial\Omega$ and $\mathbf{q} \cdot \mathbf{n}$ denotes the inner product in $\mathcal{R}^2$. The normal component $\mathbf{q} \cdot \mathbf{n}$ is understood as an element from the space $H^{-1/2}(\partial\Omega)$ and $H(\text{div}, \Omega)$ is equipped with the norm

$$||\mathbf{q}||_{H(\text{div},\Omega)} = (||\mathbf{q}||_{L^2(\Omega)^2} + ||\text{div}\mathbf{q}||_{L^2(\Omega)})^{1/2}.$$

Next, we define the trace spaces $H^{1/2}_*(\partial\Omega_k)$ as the range of the trace operator acting on $H^1_*(\Omega)$. This translates into $H^{1/2}_*(\partial\Omega_k)$ being either $H^{1/2}(\partial\Omega_k)$, if the one-dimensional measure of $\partial\Omega_k \cap \partial\Omega$ is zero, or $H^{1/2}_{00}(\partial\Omega_k \setminus \partial\Omega)$, if the measure of $\partial\Omega_k \cap \partial\Omega$ is not zero. And finally, we define $H^{-1/2}_*(\partial\Omega_k)$ to be the dual space of $H^{1/2}_*(\partial\Omega_k)$ with $< \cdot, \cdot >_{*,\partial\Omega_k}$ being the duality pairing. Often (see, e.g. [6, 7]), $H^1_0(\Omega)$ is characterized as

$$H^1_0(\Omega) = \left\{ v \in \mathcal{X} : \quad \sum_{k=1}^{K} < \mathbf{q} \cdot \mathbf{n}, v >_{*,\partial\Omega_k} = 0, \quad \mathbf{q} \in H_0(\text{div}, \Omega) \right\}. \tag{2.2}$$

Now we define the space $\mathcal{M}$ of those functions $\phi = (\phi_1, \cdots, \phi_K)$ with components $\phi_k \in H^{-1/2}_*(\partial\Omega_k)$ for $k = 1, \cdots, K$ representing traces on $\partial\Omega_k$ of a function from $H_0(\text{div}, \Omega)$, i.e.

$$\mathcal{M} = \{ \phi : \Omega_k) : \text{ iff there is } \mathbf{q} \in H_0(\text{div}, \Omega) \text{ such that for } \ k = 1, \cdots, K, \quad \phi_k = \mathbf{q} \cdot \mathbf{n}_k \}.$$

The space $\mathcal{M}$ is provided with the norm

$$||\phi||_{\mathcal{M}} = \inf \left\{ ||\mathbf{q}||_{H(\text{div},\Omega)} : \quad \mathbf{q} \in H_0(\text{div}, \Omega), \quad \mathbf{q} \cdot \mathbf{n}_k = \phi_k, \ k = 1, \cdots, K \right\}.$$

We now define the bilinear form: $B : \mathcal{X} \times \mathcal{M} \to \mathcal{R}$ by

$$B(v, \phi) = \sum_{k=1}^{K} < v_k, \phi_k >_{*,\partial\Omega_k},$$

so that the characterization (2.2) of the space $H_0^1(\Omega)$ can be written in the form:

$$H_0^1(\Omega) = \{v \in \mathcal{X}, \quad B(v, \phi) = 0, \quad \phi \in \mathcal{M}\}. \tag{2.3}$$

Further, we introduce the bilinear form $A : \mathcal{X} \times \mathcal{X} \to \mathcal{R}$ associated with the problem (2.1):

$$A(u, v) = \sum_{k=1}^{K} \int_{\Omega_k} A(x)\nabla u_k \cdot \nabla v_k dx.$$

Thus the primal hybrid formulation is of the problem (2.1) is: find $(u, \psi) \in \mathcal{X} \times \mathcal{M}$ such that

$$\begin{aligned} A(u, v) + B(v, \psi) &= (f, v), \qquad && v \in \mathcal{X}, \\ B(u, \phi) &= 0, && \phi \in \mathcal{M}. \end{aligned} \tag{2.4}$$

We have the following equivalent result:

Lemma 2.1. *(see, e.g. [6]) Problem (2.4) has a unique solution $(u, \psi) \in \mathcal{X} \times \mathcal{M}$, and the first component $u \in H_0^1(\Omega)$ is also the solution of problem (2.1). Moreover*

$$\psi_k = A\nabla u_k \cdot \mathbf{n}_k, \quad k = 1, 2, \cdots, K,$$

and

$$||u||_{H^1(\Omega)} + ||\psi||_{\mathcal{M}} \le C||f||_{L^2(\Omega)}.$$

2.2. **Finite element approximation.** Now we shall introduce the finite element approximation of the problem (2.4) studied, for example, in [6, 8, 9, 10]. We need this formulation in order to explain better the essence of the finite volume element method and to make it more transparent. Besides, in the analysis we use the theoretical tools from the above-mentioned papers or modify them according to the needs of the finite volume analysis. Each subdomain Ω_k, $k = 1, \cdots, K$ is partitioned into set $\mathcal{T}_k$ of closed triangles T so that $\overline{\Omega}_k = \cup_{T \in \mathcal{T}_k} T$. We assume that the partition $\mathcal{T}_k$ is regular (or quasi-uniform) and that any two neighboring triangles $T \in \mathcal{T}_k$ may have at most a whole common edge or a vertex. Finally, we assume that the partition is aligned with the jumps of the coefficient matrix $A(x)$. This means that over each element $T \in \mathcal{T}_k$, the elements of the matrix $A(x)$ are adequately smooth functions.

We shall also need notations for the global triangulation $\mathcal{T}_\delta$ of the domain Ω,where the size of each finite element is denoted by h_T, and the the maximal grid size in each subdomain h_k of Ω_k defined as

$$\mathcal{T}_\delta = \prod_{k=1}^{K} \mathcal{T}_k, \;\; h_T = \sup_{x,y,\in T} d(x, y), \;\; h_k = \max_{T \in \mathcal{T}_k} h_T, \;\; \delta = (h_1, \cdots, h_K).$$

The finite element spaces $\mathcal{X}_{\delta,k}$ are subspaces of $H_*^1(\Omega_k)$ of piecewise linear (over the triangulation $\mathcal{T}_k$) functions:

$$\mathcal{X}_{\delta,k} = \left\{ v_{\delta,k} \in C(\Omega_k) \cap H_*^1(\Omega_k) : \quad v_{\delta,k}|_T \in P_1(T) \right\}$$

and the global finite element space is $\mathcal{X}_\delta = \prod_{k=1}^K \mathcal{X}_{\delta,k}$., where $\delta = (h_1, \cdots, h_K)$. Note that since the grids $\mathcal{T}_k$ do not match at the subdomain interfaces Γ_{kl}, the functions in $\mathcal{X}_\delta$ are, in general, discontinuous across the interfaces. In order to ensure that the jumps in the solution u across the interfaces vanish in a weak sense, we need the space of the Lagrange multipliers. This space is the same as those introduced in the mortar finite element method (see, e.g. [6, 9, 10]). In the definition given below we use the notations from [6].

For a given integer $1 \le k \le K$ we introduce two sets $\overline{k}$ and $\underline{k}$. The latter denotes the set of integer l such that Γ_{kl} is the boundary of Ω_k with its neighboring subdomain Ω_l, while $\overline{k}$ is a subset of $\underline{k}$ of indices l such that $l > k$. These two sets will be used to introduce the space of the Lagrange multipliers. Notice that the trace of the triangulation $\mathcal{T}_k$ over Γ_{kl}, $1 \le k \le K$, $l \in \underline{k}$ results in a regular partition of Γ_{kl} denoted by t_{kl}. We shall denote the end point of this partition by $v_{1,kl}$ and $v_{2,kl}$ (these are the points a_1 and a_m on Figure 1). In general, t_{lk} differs from t_{kl} as they are induces by different triangulations $\mathcal{T}_k$ and $\mathcal{T}_l$ of the subdomains Ω_k and Ω_l which share the edge Γ_{kl}. The trace space $\mathcal{W}_{\delta,kl}$ of the functions in $\mathcal{X}_{\delta,k}$ is given by

$$\mathcal{W}_{\delta,kl} = \{\phi_{\delta,kl} \in C(\Gamma_{kl}) : \quad t \in t_{kl}, \quad \phi_{\delta,kl}|_t \text{ is a linear function}\}.$$

The finite element space of the Lagrange multipliers on a particular interface Γ_{kl}, $l > k$ (shown on Figure 1) is defined as a subspace of $\mathcal{W}_{\delta,kl}$, namely:

$$\mathcal{M}_{\delta,kl} = \{\phi_{\delta,kl} \in \mathcal{W}_{\delta,kl} : \quad t \in t_{kl}, \quad \text{or} \quad \phi_{\delta,kl}|_t \text{ is constant if } v_{1,kl} \text{ or } v_{2,kl} \in t\}.$$

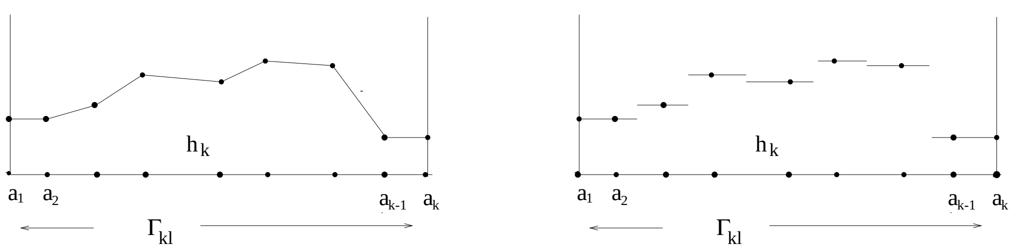

Figure 1: Function from $\mathcal{M}_k(\Gamma_{kl})$; left: piecewise linear Lagrange multipliers; right: piecewise constant Lagrange multipliers.

The finite element space for the Lagrange multipliers on all interfaces is

$$\mathcal{M}_\delta = \prod_{k=1}^{K} \prod_{l \in \overline{k}} \mathcal{M}_{\delta,kl}.$$

Remark 2.2. *The construction given above chooses the traces of finite element functions on Γ_{kl} from the subdomain Ω_k as a basis for the mortar space. This is just one possible choice of the mortar space. Other possible choice is the space of the traces of functions in the finite element space on Ω_l. One can always come up with a finite dimensional space which is not related to the partitions t_{kl} and t_{lk}. However, in this case the mortar space should not be too big or too small, since this may influence critically the accuracy of the discrete problem or the solvability of the discrete system. Namely, it should satisfy the inf-sup condition of Ladyzhenskaia, Babuska, Brezzi.*

We now define a bilinear form $B : \mathcal{X}_\delta \times \mathcal{M}_\delta \mapsto \mathcal{R}$ by

$$B(v_\delta, \phi_\delta) = \sum_{k=1}^{K} < v_{\delta,k}, \phi_{\delta,k} >_{*,\partial\Omega_k} = \sum_{k=1}^{K} \sum_{l \in \overline{k}} \int_{\Gamma_{kl}} \phi_{\delta,kl}(v_{\delta,k} - v_{\delta,l}) ds.$$

Then the *mortar finite element approximation* of (2.4) is (see, e.g. [6, 8, 9, 10]): find $u_\delta \in \mathcal{X}_\delta$ and $\psi_\delta \in \mathcal{M}_\delta$ such that

$$\begin{aligned} A(u_\delta, v_\delta) + B(v_\delta, \psi_\delta) &= (f, v_\delta), \qquad v_\delta \in \mathcal{X}_\delta, \\ B(u_\delta, \phi_\delta) &= 0, \qquad \phi_\delta \in \mathcal{M}_\delta. \end{aligned} \tag{2.5}$$

By introducing the space $\mathcal{V}_\delta$

$$\mathcal{V}_\delta = \{ v_\delta \in \mathcal{X}_\delta : \quad B(v_\delta, \phi_\delta) = 0, \quad \phi_\delta \in \mathcal{M}_\delta \},$$

the above problem can be reformulated as: find $u_\delta \in \mathcal{V}_\delta$ such that

$$A(u_\delta, v_\delta) = (f, v_\delta), \quad v_\delta \in \mathcal{V}_\delta. \tag{2.6}$$

The problems (2.5) and (2.6) are equivalent and yield stable and optimally convergent approximations of the original problem (2.1) provided that the spaces $\mathcal{X}_\delta$ and $\mathcal{M}_\delta$ are properly aligned. This approximation represents a new direction in the domain decomposition technique and has been subject to numerous studies (see, e.g. [1, 6, 8, 9, 10]).

2.3. **Finite volume element approximation.** To introduce the finite volume element method, in addition to the finite element partition $\mathcal{T}_\delta$ we shall also need the so-called finite volume (control volume or co-volume) partition $\mathcal{T}_\delta^* = \prod_{k=1}^K \mathcal{T}_k^*$ where $\mathcal{T}_k^*$ is finite volume partition of the subdomain Ω_k. This partition is described below.

First, for each k we denote by N_k the set of all vertices in the triangulation $\mathcal{T}_k$:

$$N_k = \{ p : \; p \text{ is a vertex of element } T \in \mathcal{T}_k \text{ and } p \in \overline{\Omega}_k \}.$$

In order to approximate the Dirichlet boundary conditions on $\partial\Omega$,we shall also need the set of the internal to Ω vertices, denoted by N_k^0, i.e. $N_k^0 = N_k \cap \Omega$. For a given vertex $x_{i,k}$ by $\Pi_k(i)$ we denote the subset of N_k containing the indices of all neighboring vertices of $x_{i,k}$ (neighbor means a vertex connected with $x_{i,k}$ by an edge of a triangle in $\mathcal{T}_k$).

The dual mesh $\mathcal{T}_k^*$, on which elements are called finite (control) volumes, is based upon $\mathcal{T}_k$ and can be introduced in many ways. Almost all approaches fall into the following general scheme: in each triangle $T \in \mathcal{T}_k$ a point q is selected; similarly on each edge with end points $x_{i,k}$ and $x_{j,k}$ a point $x_{ij,k}$ is chosen; then q is connected with the points $x_{ij,k}$ by straight lines splitting the element T into four quadrilateral With each vertex $x_{j,k} \in N_k$, we associate the control volume $V_{j,k} \in \mathcal{T}_k^*$, which consists of the union of the parts of T, which have $x_{j,k}$ as a vertex. Also let $\gamma_{ij,k}$ denote the interface of two adjacent control volumes $V_{i,k}$ and $V_{j,k}$: $\gamma_{ij,k} = V_{j,k} \cap V_{i,k}$, $j \in \Pi_k(i)$ (see Figure 2 and 3). If the vertex is on the interface Γ_{kl}, then "half" control volume (shaded regions, see Figure 4) is used. We shall assume that the partition $\mathcal{T}_k^*$ is quasi-uniform (or regular).

In this paper we shall use two practical ways of choosing the points q and $x_{ij,k}$, and thus determining the finite volume partition $\mathcal{T}^*$. In both case $x_{ij,k}$ is the midpoint of the edge with vertices $x_{i,k}$ and $x_{j,k}$.

In the first (and most popular) control volume partition the point q is chosen to be the medicenter (the center of gravity or centroid) of the finite element K (see Figure 2). This type of control volumes can be introduced for any finite element partition $\mathcal{T}_k$ and lead to

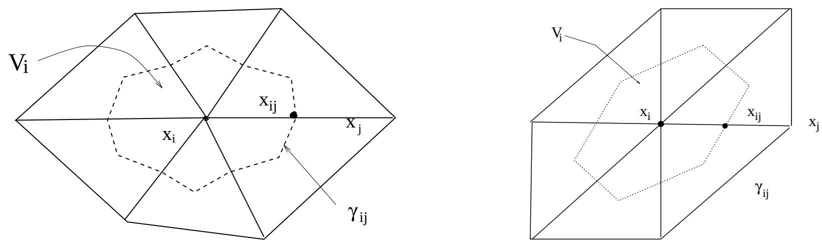

Figure 2: Control volumes with medicenters as internal point and interface γ_{ij} of V_i and V_j. The index k is omitted.

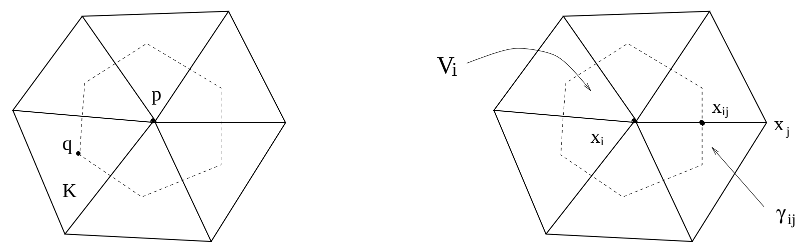

Figure 3: Control volumes with circumcenters as internal points (Voronoi meshes) and interface γ_{ij} of V_i and V_j.The index k is omitted.

relatively simple calculations. Besides, if the finite element partition $\mathcal{T}_k$ is regular then the finite volume partition $\mathcal{T}_\delta^*$ is also regular.

The second widely used finite volume partition is when the point q is chosen as the orthocenter of the finite element T. Then the edges of the finite volumes are the corresponding perpendicular bisectors of the edges of the finite elements (see Figure 3). This type of volume partition is called a Voronoi grid and has some very attractive computational features. Obviously, such co-volume partitions can be formed and will be quasi-uniform if all finite elements are acute triangles.

We define the dual space $\mathcal{X}_\delta^* = \prod_{k=1}^K \mathcal{X}_{\delta,k}^*$, where

$$\mathcal{X}_{\delta,k}^* = \{v_k \in L^2(\Omega_k) : \ v_k|_V \text{ is constant over each } \ V \in \mathcal{T}_k^* \text{ and } v_k|_{\partial\Omega\cap\partial\Omega_k} = 0\}.$$

Obviously,

$$\mathcal{X}_{\delta,k}^* = \text{span}\{\chi_{i,k} : \text{ where } \chi_{i,k} \text{ is the characteristic functions of } V_{i,k} \in \mathcal{T}_k^*\}.$$

Let $I_k : C(\Omega_k) \to \mathcal{X}_{\delta,k}$ be the standard finite element interpolation operator and $I_k^* : C(\Omega_k) \to \mathcal{X}_{\delta,k}^*$ and $P_k^* : L^2(\Omega_k) \to \mathcal{X}_{\delta,k}^*$ be the piecewise constant interpolation and L^2-projection operators, respectively:

$$I_k^* u = \sum_{i \in N_k} u_{\delta,k}(x_{i,k})\chi_{i,k}(x), \quad P_k^* u = \sum_{i \in N_k} \overline{u}_{\delta,k}(x_{i,k})\chi_{i,k}(x),$$

where

$$u_{i,k} = u(x_{i,k}) \ \text{ and } \ \overline{u}_{\delta,k}(x_{i,k}) = \frac{1}{\text{meas}(V_{i,k})} \int_{V_{i,k}} u dx.$$

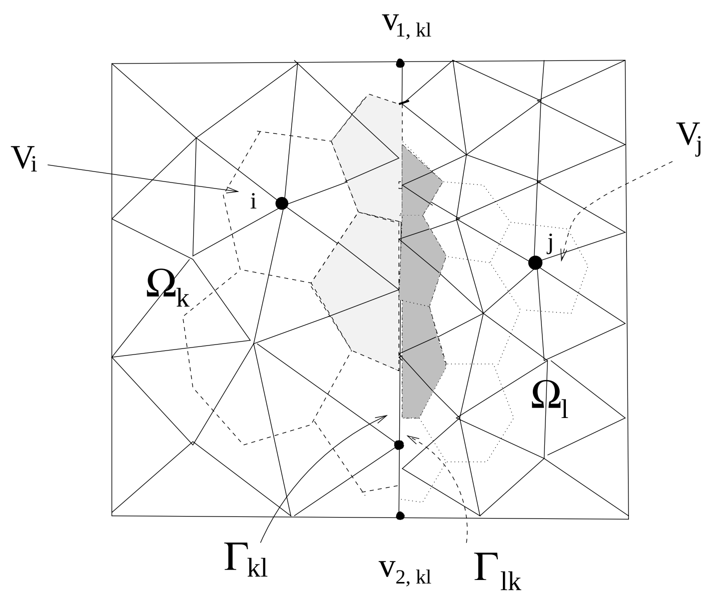

Figure 4: Interfaces Γ_{kl} and Γ_{lk} with $v_{1,kl}$ and $v_{2,kl}$ as two endpoints, Triangulation $\mathcal{T}_k$ and $\mathcal{T}_l$, and the volumes in Ω_k and Ω_l. The triangulation t_{kl} and t_{lk} are different on the interface due to non-matching grids.

Then the global interpolation and projection operators are defined as $I_\delta = \prod_{k=1}^K I_k$, $I_\delta^* = \prod_{k=1}^K I_k^*$, and $P_\delta^* = \prod_{k=1}^K P_k^*$.

The *mortar finite volume element method* is : find $(u_\delta, \psi_\delta) \in \mathcal{X}_\delta \times \mathcal{M}_\delta$ such that

$$
\begin{aligned}
A(u_\delta, I_\delta^* v_\delta) + B(v_\delta, \psi_\delta) &= (f, I_\delta^* v_\delta), \quad v_\delta \in \mathcal{X}_\delta, \\
B(v_\delta, \phi_\delta) &= 0, \qquad\qquad\quad \phi_\delta \in \mathcal{M}_\delta,
\end{aligned} \tag{2.7}
$$

where

$$
\begin{aligned}
A(u_\delta, I_\delta^* v_\delta) &= -\sum_{k=1}^K \sum_{j \in N_k^0} v_{\delta,k}(x_{j,k}) \int_{\partial V_{j,k} \setminus \partial\Omega_k} A(x) \nabla u_{\delta,k} \cdot \mathbf{n}_k ds, \\
(f, I_\delta^* v_\delta) &= \sum_{k=1}^K \sum_{j \in N_k^0} v_{\delta,k}(x_{j,k}) \int_{V_{j,k}} f(x) dx.
\end{aligned}
$$

This problem is equivalent to the following one: find $u_\delta \in \mathcal{V}_\delta$ such that

$$
A(u_\delta, I_\delta^* v_\delta) = (f, I_\delta^* v_\delta), \quad v_\delta \in \mathcal{V}_\delta. \tag{2.8}
$$

Remark 2.3. *This construction leads in general to non-conforming finite element spaces $\mathcal{V}_\delta$, i.e. $\mathcal{V}_\delta$ is not a subspace of $H_0^1(\Omega)$. However, this does not degrade the overall rate of convergence of the method.*

Note, that in contrast to the standard mortar Galerkin finite element method (2.5) the bilinear form of the finite volume element method $A(u_\delta, I_\delta^* v_\delta)$ is in general non-symmetric since it is defined on two different spaces $\mathcal{X}_\delta \times \mathcal{X}_\delta^*$. This will lead to nonsymmetric algebraic problems since the global stiffness matrix is assembled from the local matrices which, in general, are nonsymmetric. However, if the coefficient matrix $A(x)$ is constant over each finite element T, then the mortar finite volume element methodintroduced above coincides with the the standard mortar Galerkin finite element method with piecewise linear elements studied, for example, in [6, 9, 10]. This is due to the fact, established in [20] (see, also [15, 22, 23]):

Lemma 2.2. *Assume that the matrix $A(x)$ is constant on each $T \in \mathcal{T}_k$ for $k = 1, \cdots, K$. Then*

$$A(u_\delta, v_\delta) = A(u_\delta, I_\delta^* v_\delta), \quad \forall u_\delta,\ v_\delta \in \mathcal{X}_\delta. \tag{2.9}$$

Therefore, for piecewise constant coefficients, the mortar finite element and finite volume approximations produce the same element stiffness matrices. The difference in the stiffness matrix occurs where the coefficients vary in the finite elements. This method will prduce a different mass matrix and right-hand side, but for smooth coefficients they are only $O(h^2)$ perturbations of the finite element conterparts. Later we discuss various other possible mortar finite volume approximations (see Remark 2.4 below and Section 4).

Obviously, the weak interface continuity in the mortar finite volume element method is imposed in the same way as in the finite element method since they both use piecewise linear test functions for the Lagrange multipliers. Thus, the weak compatibility condition of the spaces $\mathcal{X}_\delta$ and $\mathcal{M}_\delta$ is satisfied automatically:

$$\{\phi_\delta : \quad B(v_\delta, \phi_\delta) = 0, \quad \forall v_\delta \in \mathcal{X}_\delta\} = \{0\}. \tag{2.10}$$

However, continuous linear test functions for the interface condition will not preserve the basic feature of finite volume element method – its local mass conservation property. More precisely, this formulation leads to locally conservative approximations only for the volumes that are internal with respect to the subdomains Ω_k. For volumes centered at points on the interface boundaries Γ_{kl}, this formulation is not locally conservative.

Remark 2.4. *One can also write a mortar approximation, which is locally conservative for all volumes: find $(v_\delta, \psi_\delta) \in \mathcal{X}_\delta \times \mathcal{M}_\delta$ such that*

$$\begin{aligned} A(u_\delta, I_\delta^* v_\delta) + B(I_\delta^* v_\delta, \psi_\delta) \quad &= (f, I_\delta^* v_\delta), \qquad v_\delta \in \mathcal{X}_\delta, \\ B(I_\delta^* u_\delta, \phi_\delta) \quad &= 0, \qquad\qquad\quad \phi_\delta \in \mathcal{M}_\delta. \end{aligned} \tag{2.11}$$

This simple approach will also preserve the symmetry in treating the interface conditions. Other approximations will be discussed in Section 4.

3. Optimal order H^1-error estimates

In this section we establish the main theoretical result of the paper: existence and uniqueness of the solution of the mortar finite volume element method (2.7) and establish optimal order error estimate for the solution u_δ. Our analysis uses the mathematical technique developed in [6, 9, 10] with the necessary modifications for the finite volume.

Note, that $||u_\delta||_{\mathcal{X}_\delta}$ is a semi-norm in $\mathcal{X}_\delta$ and a norm in $\mathcal{V}_\delta$. Now we prove the following lemma:

Lemma 3.1. *There exists $C_1 > 0$, independent of δ, such that*

$$|A(u_\delta, I_\delta^* v_\delta)| \le C_1 |u_\delta|_{\mathcal{X}} |v_\delta|_{\mathcal{X}}, \quad u_\delta, v_\delta \in \mathcal{X}_\delta. \tag{3.1}$$

Besides, if δ is sufficiently small (which translates in smallness of h_k, $k = 1, \cdots, K$) then there is a constant $C_0 > 0$, independent of δ, such that

$$A(u_\delta, I_\delta^* u_\delta)| \geq C_0 |u_\delta|_{\mathcal{X}}^2, \quad u_\delta \in \mathcal{X}_\delta. \tag{3.2}$$

Proof: Since

$$\begin{aligned} A(u_\delta, I_\delta^* v_\delta) &= -\sum_{k=1}^{K} \sum_{j \in N_k^0} v_{\delta,k}(x_{j,k}) \int_{\partial V_{j,k} \setminus \partial \Omega_k} A(x) \nabla u_{\delta,k} \cdot \mathbf{n} ds, \\ &= -\frac{1}{2} \sum_{k=1}^{K} \sum_{j \in N_k^0} \sum_{i \in \Pi_k(j)} \int_{\gamma_{ij,k}} A(x) \nabla u_{\delta,k} \cdot \mathbf{n} ds (v_{\delta,k}(x_{i,k}) - v_{\delta,k}(x_{j,k})). \end{aligned}$$

Since the squared norm of $\nabla u_{\delta,k}$ over each element is equivalent to the sum of the squared differences of the values of $u_{\delta,k}$ at the vertices of the element, the inequality (3.1) follows immediately. To show (3.2), we first define the mean values of the matrix $A(x)$ over each finite volume

$$\overline{A}(x) = \frac{1}{\text{meas } T} \int_T A(y) dy, \quad \text{if} \quad x \in T, \quad T \in \mathcal{T}_k, \quad 1 \leq k \leq K. \tag{3.3}$$

Using Lemma 2.2 we easily get the following equality:

$$\begin{aligned} A(u_\delta, I_\delta^* u_\delta) &= -\sum_{k=1}^{K} \sum_{j \in N_k^0} u_{\delta,k}(x_{j,k}) \int_{\partial V_{j,k} \setminus \partial \Omega_k} (A(x) - \overline{A}(x)) \nabla u_{\delta,k} \cdot \mathbf{n}_k ds \\ &\quad + \sum_{k=1}^{K} \sum_{T \in \mathcal{T}_k} \int_T (\overline{A}(x) - A(x)) \nabla u_{\delta,k} \cdot \nabla u_{\delta,k} dx \\ &\quad + \sum_{k=1}^{K} \sum_{T \in \mathcal{T}_k} \int_T A(x) \nabla u_{\delta,k} \cdot \nabla u_{\delta,k} dx. \end{aligned}$$

$A(x)$ is smooth over each element K and, therefore. $|A(x) - \overline{A}(x)| \leq C h_k$ for $x \in \Omega_k$ for $k = 1, \cdots, K$. Since the last term is positive definite, we get

$$A(u_\delta, I_\delta^* u_\delta) \geq C \sum_{k=1}^{K} \left(|u_{\delta,k}|_{H^1(\Omega_k)}^2 - C h_k |u_{\delta,k}|_{H^1(\Omega_k)}^2 \right)$$

from which (3.2) follows for sufficiently small h_k, $k = 1, \cdots, K$.

Lemma 3.2. *Assume that the solution u of the problem (2.1) belong to the space $H^{1+\tau_k}(\Omega_k)$ with $\tau_k > 0$ for $k = 1, \cdots, K$. Then the following estimate holds true:*

$$\sup_{0 \neq v_\delta \in \mathcal{V}_\delta} \frac{(f, v_\delta) - A(u, v_\delta)}{||v_\delta||_{\mathcal{X}}} \leq C \sum_{k=1}^{K} h_k^{\tau_k} ||u||_{H^{1+\tau_k}(\Omega_k)}. \tag{3.4}$$

Proof: See [6, 7].

Theorem 3.1. *The problem (2.7) has unique solution* (u_δ, ψ_δ) *in* $\mathcal{X}_\delta \times \mathcal{M}_\delta$. *(2.7). Moreover, if* $u \in H^{1+\tau_k}(\Omega_k)$ *for some* $\tau_k > 0$, $k = 1, \cdots, K$, *then* u_δ *coincides with the solution of (2.8) and satisfies the following error estimate:*

$$||u - u_\delta||_{\mathcal{X}} \le C \sum_{k=1}^{K} \left(h_k^{\tau_k} ||u||_{H^{1+\tau_k}(\Omega_k)} + h_k ||f||_{L^2(\Omega_k)} \right) \tag{3.5}$$

with a constant $C > 0$ *independent of* $\delta = (h_1, \cdots, K)$.

Proof: The existence and uniqueness follows from the inequality (3.2) of Lemma 3.1 and compatibility condition (2.10). Also, we know that the solution u_δ is stable with respect to the right hand side, so it satisfies the *a priori* estimate: $||u_\delta||_{\mathcal{X}_\delta} \le C||f||$.

As for the error estimates, we rewrite the first equation of (2.7) in the form: argument above:

$$A(u_\delta, v_\delta) + B(v_\delta, \psi_\delta) \quad = \quad (f, v_\delta) + r_\delta(v_\delta) + R_\delta(u_\delta, v_\delta), \tag{3.6}$$

where

$$\begin{aligned} r_\delta(v_\delta) \quad &= \quad (f, I_\delta^* v_\delta - v_\delta), & (3.7)\\ R_\delta(u_\delta, v_\delta) \quad &= \quad -\sum_{k=1}^{K} \sum_{j \in N_k^0} v_{\delta,k}(x_{j,k}) \int_{\partial V_{j,k} \setminus \partial \Omega_k} (A(x) - \overline{A}(x)) \nabla u_{\delta,k} \cdot \mathbf{n}_k ds \\ &\quad + \sum_{k=1}^{K} \sum_{T \in \mathcal{T}_k} \int_T (\overline{A}(x) - A(x)) \nabla u_{\delta,k} \cdot \nabla v_{\delta,k} dx. & (3.8) \end{aligned}$$

Thus second Strang's Lemma implies that (see, e.g. [6, 26]):

$$\begin{aligned} ||u - u_\delta||_{\mathcal{X}} \quad \le \quad & C \left(\inf_{v_\delta \in \mathcal{V}_\delta} ||u - v_\delta||_{\mathcal{X}} + \sup_{0 \ne v_\delta \in \mathcal{V}_\delta} \frac{r_\delta(v_\delta) + R_\delta(u_\delta, v_\delta)}{|v_\delta|_{\mathcal{X}}} \right. \\ & \left. + \inf_{\psi_\delta \in \mathcal{M}_\delta} \sup_{0 \ne v_\delta \in \mathcal{V}_\delta} \frac{B(v_\delta, \psi - \psi_\delta)}{|v_\delta|_{\mathcal{X}}} \right). \end{aligned} \tag{3.9}$$

Clearly,

$$\begin{aligned} r_\delta(v_\delta) + R_\delta(u_\delta, v_\delta) \quad &\le \quad C \sum_{k=1}^{K} h_k \big(||f||_{L^2(\Omega_k)} \, |v_{\delta,k}|_{H^1(\Omega_k)} + |u_{\delta,k}|_{H^1(\Omega_k)} \, |v_{\delta,k}|_{H^1(\Omega_k)} \big) \\ &\le \quad C |v_\delta|_{\mathcal{X}} \sum_{k=1}^{K} h_k \left(||f||_{L^2(\Omega_k)} + ||u||_{H^1(\Omega_k)} \right). \end{aligned}$$

Also, for $v_\delta \in \mathcal{V}_\delta$ and $\phi_\delta \in \mathcal{M}_\delta$, we have

$$\begin{aligned} B(v_\delta, \psi - \phi_\delta) \quad &= \quad B(v_\delta, \psi) \\ &= \quad (f, v_\delta) - A(u, v_\delta), \end{aligned}$$

thus, by from Lemma 3.2 we get

$$|B(v_\delta, \psi - \phi_\delta)| \le C \left(\sum_{k=1}^{K} h_k^{\tau_k} ||u||_{H^{1+\tau_k}(\Omega_k)} \right) |v_\delta|_{\mathcal{X}}.$$

Hence (3.5) follows.

4. Extensions and generalizations

4.1. **Piecewise constant approximations on interfaces.** Here we shall use a modification $\mathcal{M}_\delta^*$ of the mortar finite element space $\mathcal{M}_\delta$ so the new space better reflects the conservation properties of the finite volume element method while it preserves the order of approximation of the unknown solution. Namely, the Lagrange multipliers ψ on Γ_{kl} are approximated by piecewise constant functions over a finite volume partition of Γ_{kl}. $\mathcal{X}_{\delta,k}^*$. This new space is defined as $\mathcal{M}_\delta^* = \prod_{k=1}^K \prod_{l\in\overline{k}} \mathcal{M}_{\delta,kl}^*$, where the spaces $\mathcal{M}_{\delta,kl}^*$ for $l \in \overline{k}$ are constructed in the following way. Let t_{kl} be the partition of interface Γ_{kl} induced by the triangulation $\mathcal{T}_k$ and $v_{1,kl}$ and $v_{2,kl}$ be the end points of Γ_{kl}. Then $\mathcal{M}_{\delta,kl}^*$ consists of the modified traces of functions from $\mathcal{X}_{\delta,kl}^*$. The modification is done only for the two volumes corresponding to the endpoints $v_{1,kl}$ and $v_{2,kl}$, where a constant value is prescribed equal to the value at the adjacent internal nodal points (see Figure 1).

Now we can introduce two additional mortar finite element approximations of the original problem (2.1): find a pair $(u_\delta, \psi_\delta^*) \in \mathcal{X}_\delta \times \mathcal{M}_\delta^*$ such that

$$\begin{array}{lcll} A(u_\delta, I_\delta^* v_\delta) + B(v_\delta, \psi_\delta^*) & = & (f, I_\delta^* v_\delta), & v_\delta \in \mathcal{X}_\delta, \\ B(u_\delta, \phi_\delta^*) & = & 0, & \phi_\delta^* \in \mathcal{M}_\delta^*, \end{array} \tag{4.1}$$

or

$$\begin{array}{lcll} A(u_\delta, I_\delta^* v_\delta) + B(I_\delta^* v_\delta, \psi_\delta^*) & = & (f, I_\delta^* v_\delta), & v_\delta \in \mathcal{X}_\delta, \\ B(I_\delta^* u_\delta, \phi_\delta^*) & = & 0, & \phi_\delta^* \in \mathcal{M}_\delta^*. \end{array} \tag{4.2}$$

As it can be checked easily that

$$\{\phi_\delta^* \in \mathcal{M}_\delta^* : \quad B(v_\delta, \phi_\delta^*) = 0, \quad \forall v_\delta \in \mathcal{X}_\delta\} = \{0\}, \tag{4.3}$$

$$\{\phi_\delta^* \in \mathcal{M}_\delta^* : \quad B(I_\delta^* v_\delta, \phi_\delta^*) = 0, \quad \forall v_\delta \in \mathcal{X}_\delta\} = \{0\}. \tag{4.4}$$

These two facts imply that both problems (4.1) and (4.2) have unique solution pairs $(u_\delta, \psi_\delta) \in \mathcal{X}_\delta \times \mathcal{M}_\delta^*$, and the error bounds (3.5) hold for both problems. Namely, the following result is valid:

Theorem 4.1. *The problems (4.1) and (4.2) have unique solutions $(u_\delta, \psi_\delta^*) \in \mathcal{X}_\delta \times \mathcal{M}_\delta^*$, correspondingly, and if $u \in H^{1+\tau_k}(\Omega_k)$ for $\tau_k > 0$, $k = 1, \cdots, K$, then the following error estimates are valid:*

$$||u - u_\delta||_{\mathcal{X}} \le C \sum_{k=1}^K \Big(h_k^{\tau_k} ||u||_{H^{1+\tau_k}(\Omega_k)} + h_k ||f||_{L^2(\Omega_k)} \Big). \tag{4.5}$$

Proof: See the analysis above.

4.2. **Combination of various other approximations.** First, we propose an approximation scheme using combined finite element and finite volume element methods. To simplify the presentation, we assume that the domain is divided into two subdomains: $\Omega = \Omega_1 \cup \Omega_2$ with $\Gamma_{12} = \partial\Omega_1 \cap \partial\Omega_2$ so that linear finite elements are used in Ω_1 and linear finite volume elements in Ω_2.

Thus, the combined finite element and finite volume element approximations are: find $(u_\delta, \psi_\delta) \equiv (u_{\delta,1}, v_{\delta,2}, \psi_\delta) \in \mathcal{X}_\delta \times \mathcal{M}_\delta$ such that

$$
\begin{array}{llcll}
A_{\Omega_1}(u_{\delta,1}, I_1^* v_{\delta,1}) & + \; B(v_{\delta,1}, \psi_\delta) & = & (f, I_1^* v_{\delta,1})_{\Omega_1}, & v_{\delta,1} \in \mathcal{X}_{\delta,1}, \\
A_{\Omega_2}(u_{\delta,2}, v_{\delta,2}) & + \; B(v_{\delta,2}, \psi_\delta) & = & (f, v_{\delta,2})_{\Omega_2}, & v_{\delta,2} \in \mathcal{X}_{\delta,2}, \\
B(u_\delta, \phi_\delta) & & = & 0, & \phi_\delta \in \mathcal{M}_\delta.
\end{array} \tag{4.6}
$$

where A_{Ω_i} and $(\cdot,\cdot)_{\Omega_i}$ denote the bilinear forms and the inner product on the subdomains Ω_i, $i = 1, 2$, correspondingly.

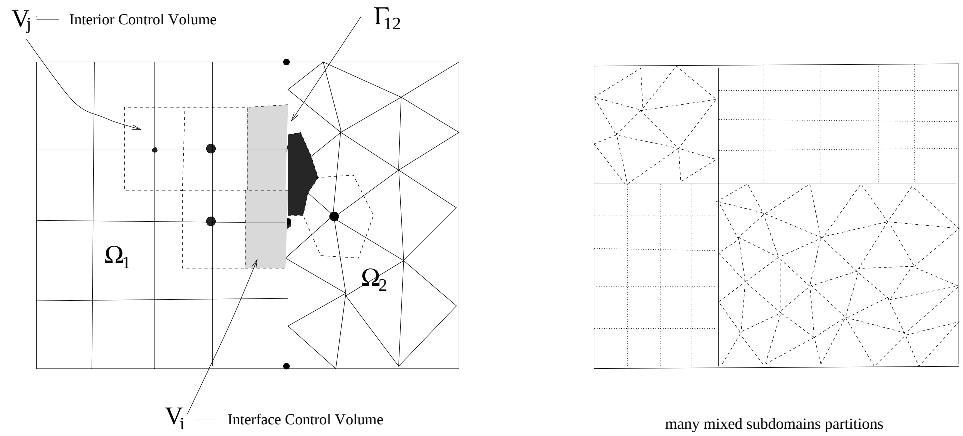

Figure 5: Left: Rectangular and triangular grids on two different subdomains. Right: General rectangular and triangular partitions on subdomains.

Next, we describe a method that combines the rectangular and triangular girds on different subdomains. For simplicity, we consider only two subdomains (see Figure 5). with bilinear finite elements in Ω_1 and linear finite elements in Ω_2. The piecewise constant interpolation operator $I_1^* : C(\Omega) \to \mathcal{X}_\delta$ is defined in the standard way so $I_1^* u|_{V_j} = u(x_j)$ and $I_1^* u|_{V_j} = \int_{V_j} u dx / \text{meas}(V_j)$ for all internal volumes and zero at the boundary control volumes.

Thus, the finite volume element approximation is: find $(u_\delta, \phi_\delta) \in \mathcal{X}_\delta \times \mathcal{M}_\delta$ such that (4.6) is satisfied. Note, that $\mathcal{X}_\delta$ is different from the one used in Section 4.2.

Finally, one can formulate and study approximation schemes by using geometrically nonconforming subdomain partitions (see Fugure 6).

All suggested schemes are stable and approximate the solution of the original problem (2.1) so that estimates similar to that of Theorem 3.1 are valid.

5. Numerical Examples

In this section, we report some numerical results yielded by the mortar finite volume element method. Two specific boundary value problems are considered. In both problems, the solution domain Ω can be separated into two subdomains $\Omega = \Omega_1 \cup \Gamma_{12} \cup \Omega_2$ such that the solution changes much more dramatically in Ω_1 than in Ω_2. The data functions for the first problem are smooth, while the second problem has a discontinuous coefficient. Domain

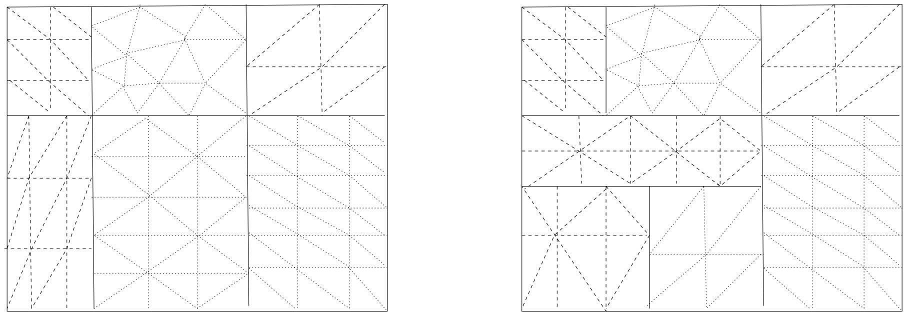

Figure 6: Left: Geometrically conforming subdomain division. Right: Geometrically nonconforming subdomain partition.

decomposition is therefore employed to separate Ω_1 from Ω_2 so that the fine grid used in Ω_1 has a numerical approximation with enough accuracy to match the accuracy on Ω_2 obtained on a coarser grid.

We measure the error $e_\delta = u_\delta - u$ in the discret $L^\infty-$, L^2-, and H^1-norms defined by:

$$||e_\delta||_{L^\infty} = \max_{(x_i,y_j)} |u_\delta(x_i,y_j) - u(x_i,y_j)|,$$

$$||e_\delta||^2_{H^s(\Omega)} = \sum_{T\in\mathcal{T}_\delta} ||e_\delta||^2_{H^s(T)},\ s = 0,1,$$

where numerical quadrature formulas are used evaluate the integrals over the element T. Finally, the Uzawa algorithm with conjugate directions is used to solve the corresponding linear system.

Example 1: We consider the problem (2.1) with $\Omega = (0,1)^2$ and $A(x) \equiv I$ and the forcing term $f(x)$ i chosen in such a way that the exact solution is

$$u(x,y) = bx(e^{ax} - e^a)y(e^{ay} - e^a),\ a = 13, b = 0.90909 \times 10^{11}.$$

This solution obviously changes substantially in the upper right conner of the domain Ω. We therefore separate Ω into two subdomains $\Omega_1 = (0.5,1)\times(0.5,1)$ and Ω_2 is the remaining part of Ω. All results presented for this example are obtained using piecewise bilinear functions over the rectangular partition of Ω_1 and piecewise linear functions over the triangulation of Ω_2. Both partitions $\mathcal{T}_1$ of Ω_1 and $\mathcal{T}_2$ of Ω_2 are uniform and the grid size in Ω_2 is always four times larger than the grid size in Ω_1. Figure 7 shows a typical grid used in the computation for this example. The partition used for the Lagrange multipliers space can be the restriction of either partition $\mathcal{T}_1$ or $\mathcal{T}_2$ on the interface of Ω_1 and Ω_2.

Tables 1 and 2 contain the numerical results by using linear finite element functions for the multiplier on a grids induced by the partition in Ω_2 and Ω_1, respectively. The reduction in the grid size and error indicates that the method seems to converge in the first order in H^1-norm, and in the second order in L^2-norm. Table 3 contains similar numerical results for piecewise constant finite element functions used for the Lagrange multipliers on a grids induced by the partition in Ω_2. These results also indicate that the convergence of the method is first order in H^1-norm, and second order in L^2-norm.

Using the grid induced from the fine partition in Ω_1 will impose more constraints on the finite element spaces in both Ω_1 and Ω_2, and this can make the method less accurate if the

h	$\|e_h\|_{H^1(\Omega)}$	$\|e_h\|_{L^2(\Omega)}$	$\|e_h\|_{L^\infty(\Omega)}$	number of iterations
1/10	7.2837×10^{-1}	2.8265×10^{-2}	8.2126×10^{-2}	4
1/20	3.7258×10^{-1}	7.5642×10^{-3}	2.5478×10^{-2}	11
1/40	1.8700×10^{-1}	1.9242×10^{-3}	6.8271×10^{-3}	29
1/80	9.3539×10^{-2}	4.8315×10^{-4}	1.7155×10^{-3}	50

Table 1: Errors for Example 1. The Lagrange multiplier space consists of piecewise linear finite functions on a grid induced from the partition in the domain Ω_2, where a coarse grid with step-size h is used.

h	$\|e_h\|_{H^1(\Omega)}$	$\|e_h\|_{L^2(\Omega)}$	$\|e_h\|_{L^\infty(\Omega)}$	number of iterations
1/10	7.4240×10^{-1}	2.8762×10^{-2}	1.2535×10^{-1}	32
1/20	3.7651×10^{-1}	7.6449×10^{-3}	4.0114×10^{-2}	72
1/40	1.8804×10^{-1}	1.9353×10^{-3}	1.1124×10^{-2}	113
1/80	9.3803×10^{-2}	4.8457×10^{-4}	2.8898×10^{-3}	156

Table 2: Errors for Example 1. The Lagrange multiplier space is formed by the linear finite element in a grid induced from the partition in the domain Ω_1.

ratio of the grid sizes in Ω_2 and Ω_1 is too large a fact obsereved in the results presented in Table 4. It seems that the convergence is slower compared with those in the previous tables. Note that the grid size h listed in all of these tables is for the coarse grid in Ω_2. Also, using the partition induced from the coarse partition in Ω_2 for the Lagrange multipliers space requires much less iterations needed to solve the corresponding linear system (see Table 1 and Table 2).

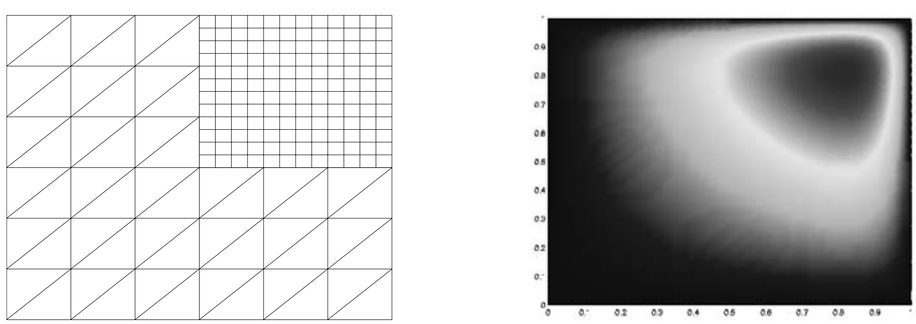

Figure 7: Left: a typical grid for Example 1. Right: the numerical solution generated by the mortar finite volume element method.

Example 2: We consider the problem (2.1) with $\Omega = \{(x_1, x_2) : 0 < x_1 < 1,\ -1 < x_2 < 1\}$, the coefficient matrix $A(x) = a(x)I$, where

$$a(x) = \begin{cases} \beta_1, & \text{if } x_2 < 0, \\ \beta_2, & \text{if } x_2 > 0, \end{cases}$$

h	$\|e_h\|_{H^1(\Omega)}$	$\|e_h\|_{L^2(\Omega)}$	$\|e_h\|_{L^\infty(\Omega)}$	number of iterations
1/10	7.2967×10^{-1}	2.8611×10^{-2}	8.1079×10^{-2}	4
1/20	3.7711×10^{-1}	7.6871×10^{-3}	3.6196×10^{-2}	11
1/40	1.9058×10^{-1}	1.9761×10^{-3}	1.7306×10^{-2}	22
1/80	9.5691×10^{-2}	5.0325×10^{-4}	8.6610×10^{-3}	31

Table 3: Errors for Example 1. The Lagrange multiplier space is formed by the zero-th degree finite element in a grid induced from the partition in the domain Ω_2.

h	$\|e_h\|_{H^1(\Omega)}$	$\|e_h\|_{L^2(\Omega)}$	$\|e_h\|_{L^\infty(\Omega)}$	number of iterations
1/10	8.1802×10^{-1}	3.5424×10^{-2}	2.4033×10^{-1}	21
1/20	4.5596×10^{-1}	1.1388×10^{-3}	1.3157×10^{-1}	32
1/40	2.6406×10^{-1}	3.9800×10^{-3}	6.8890×10^{-2}	44
1/80	1.61960×10^{-1}	1.5789×10^{-4}	3.5255×10^{-2}	60

Table 4: Errors for Example 1. The Lagrange multiplier space is formed by the zero-th degree finite element in a grid induced from the partition in the domain Ω_1.

and the forcing term $f(x, y)$ is chosen such a way that the following function is exact solution to this problem:

$$\begin{aligned} u(x) &= \begin{cases} sin(\pi x_1)(x_2+1)(x_2+b_2)/\beta_1, \text{if } x_2 < 0, \\ sin(\pi x_1)(x_2-1)(x_2+b_1)/\beta_2, \text{if } x_2 > 0, \end{cases} \\ b_2 &= -2/(1+\frac{\beta_2}{\beta_1}),\ b_1 = -\frac{\beta_2}{\beta_1} b_2. \end{aligned}$$

We have run our experiments with $\beta_2 = 100\beta_1 = 100$. The coefficient is discontinuous along the line $x_2 = 0$ which separates the domain into two subdomains. The exact solution is rather flat in the top half of the subdomain Ω_2. Some numerical results are listed in the Table 5, which are obtained by using bilinear finite element functions in both Ω_1 and Ω_2, but piecewise constant finite element functions for the multiplier on the interface. Figure 8 shows a typical grid for this example. The grid size in Ω_2 is always chosen five times as large as that used in Ω_1. Again, the reduction in the grid size and error indicates that the convergence is first order in H^1-norm, and second order in L^2-norm.

References

[1] Y. Achdou, Y. Maday, and O. Widlund, *Iterative substructuring preconditioners for mortar element methods in two dimensions*, *SIAM J. Numerical Analysis*, **36**(1999), pp. 551–580.

[2] M. A. Aminpour, S. L. McClearly, J. B. Ransom, *A global/local analysis method for treating details in structural design*, Proc. Third NASA Adv. Composites Tech. Conf., NASA CP-3178, vol. 1, part 2, 1992, 967-986.

[3] G. Anagnostou, Y. Maday, C. Mavriplis, and A. Patera, *On the mortar element method: generalization and implementation*, Proc. Third Int. Conf. on Domain Decomposition Methods for PDEs, T. Chan et al eds., SIAM Philadelphia, 1990.

[4] T. Arbogast and I. Yotov, *A non-mortar mixed finite element method for elliptic problems on non-matching multi-block grids*, Comp. Meth. in Appl. Mech. and Engng., **149** (1997) 255–265.

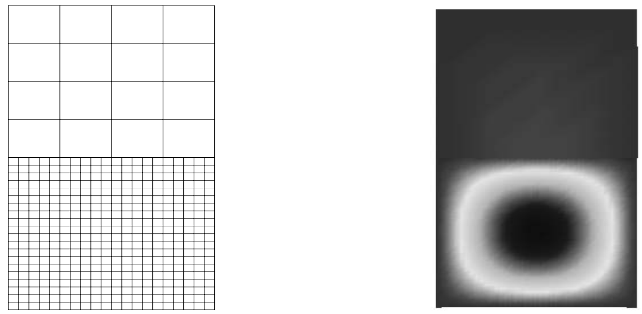

Figure 8: Left: a typical grid for Example 1; right: the numerical solution generated by the mortar finite volume element method.

h	$\|e_h\|_{H^1(\Omega)}$	$\|e_h\|_{L^2(\Omega)}$	$\|e_h\|_{L^\infty(\Omega)}$	number of iterations
1/10	5.8344×10^{-2}	2.6846×10^{-3}	2.1669×10^{-2}	2
1/20	2.1330×10^{-2}	3.8058×10^{-4}	6.2210×10^{-3}	4
1/40	8.6550×10^{-3}	5.5916×10^{-5}	1.7132×10^{-3}	9
1/80	3.9203×10^{-3}	9.9364×10^{-6}	5.0792×10^{-4}	15

Table 5: Errors for Example 2. The space of the Lagrange multipliers consists of discontinuous pice-wise constant functions on a grid induced from the partition in the domain Ω_2.

[5] B.R. Baliga and S.V. Patankar, *A new finite-element formulation for convection-diffusion problems*, Numer. Heat Transfer, **3** (1980), 393–409.

[6] F. Ben Belgacem, *The mortar finite element method with Lagrange multiplier*, Numer. Math., **84** (1999), 173–197.

[7] F. Ben Belgacem and Y. Maday, *Nonconforming spectral element methodology tuned to parallel implementation,* Comput. Meth. Appl. Mech. Eng., **116** (1994), 59-67.

[8] C. Bernardi, Y. Maday, and Y. Achdou, *The mortar element method for three dimensional finite elements*, M2NA, **31** (1997) 289-301.

[9] C. Bernardi, N. Debit and Y. Maday, *Coupling finite element and spectral methods: First results,* Math. Comp. **54** (1990), 21-39.

[10] C. Bernardi, Y. Maday and A. Patera, *A new non conforming approach to domain decomposition: The mortar element method*, Nonlinear Partial Differential Equations and Their Applications, (H. Brezis and J.L Lions, eds), Pitman Research Notes in Math. Series 299, Longman 1994, 13–51 (appeared in 1989 as Technical Report).

[11] C. Bernardi, Y. Maday, and G. Sacchi-Landriani, *Nonconforming matching conditions for coupling spectral finite element methods*, Appl. Numer. Math., **54** (1989), 64-84.

[12] F. Brezzi and D. Marini, *Macro hybrid elements and domai decomposition methods*, Proc. Colloque en l'honeur du 60-eme anniversaire de Jean Cea, Sophia-Antipolis, 1992.

[13] F. Brezzi and M. Fortin, *Mixed and Hybrid Finite Element Methods*, Springer-Verlag, 1991.

[14] Z. Cai, J. J. Jones, S. F. McCormick, and T. F. Russell, *Control-volume mixed finite element methods*, Computational Geosciences, **1** (1997) 289–315.

[15] Z. Cai and S. McCormick, *On the accuracy of the finite volume element method for diffusion equations on composite grids*, SIAM J. Numer. Anal., **27** (1990), 636-655.

[16] S.H. Chou and P.S. Vassilevski, *A general mixed co-volume framework for constructing conservative schemes for elliptic problems,* Manuscript 1997, Math. Comp., **68** (1999) (to appear).

[17] M. Dorr, *A domain decomposition preconditioner with reduced rank interdomain coupling,* Appl. Numer. Math., **8** (1991) 333–352.

[18] R.E. Ewing, R.D. Lazarov, and Y. Lin, *Finite volume element approximations of nonlocal reactive transport flows in porous media*, *Technical Report ISC-98-07-MATH* (to apper in Numer. Meth. PDEs).

[19] R.E. Ewing, R.D. Lazarov, T. Lin, and Y. Lin, *Domain decomposition capabilities for the mortar finite volume element methods*, 11-th International Conference on Domain Decomposition Methods in Science and Engineering, London, 1998, C.H. Lai, P.E. Bjorstad, M. Cross, and O.Widlund, Eds, DD Press, Bergen, 1999, pp. 220–227.

[20] H. Jianguo and X. Shitong, *On the finite volume element method for general self-adjoint elliptic problems,* SIAM J. Numer. Anal., **35** (1998), 1762-1774.

[21] R.H. Li and Z.Y. Chen, *The Generalized Difference Method for Differential Equations*, Jilin University Publishing House, 1994.

[22] I.D. Mishev, *Finite volume and finite volume element methods for non-symmetric problems*, Texas A&M University, Ph.D. thesis, 1997, Technical Report ISC-96-04-MATH.

[23] I.D. Mishev, *Finite Volume Methods on Voronoi Meshes*, Numerical Methods for Partial Differential Equations, **14** (1998), 193-212.

[24] A.A. Samarskii, *Theory of the Difference Schemes*, Moscow, Nauka, 1977.

[25] P.A. Raviart and J.M. Thomas, *A mixed finite element method for 2nd order elliptic problems*, Mathematical Aspects of Finite Element Methods (I. Galligani and E. Magenes, eds), Lecture Notes in Math., **606**, Springer-Verlag, Berlin and New York, (1977), 292-315.

[26] P.A. Raviart and J.M. Thomas, *Primal hybrid finite element methods for second order elliptic equations*, Math. Comp., 31 (1977), 391–396.

[27] H. Swan, *On the use of Lagrange multipliers in domain decomposition for solving elliptic problems*, Math. Comp., **60** (1993) 49–78.

[28] P. Seshaiyer and M. Suri, *Uniform $h-p$ convergence results for the mortar finite element method*, Preprint 1998 (to appear in Math. Comp.).

[29] C. Wiener and B. Wohlmuth, *Coupling of mixed and conforming finite element discretizations*, American Mathematical Society, Cont. Math. 218 (1998), 547–554.

Institute for Scientific Computation, Texas A&M University, College Station, TX 77843-3404
E-mail address: `ewing@isc.tamu.edu`

Department of Mathematics, Texas A&M University, College Station, TX 77843-3368
E-mail address: `lazarov@math.tamu.edu`

Department of Mathematics, Virginia Tech, Blackburg, VA 24061
E-mail address: `tlin@calvin.math.vt.edu`

Department of Mathematics, University of Alberta, Edmonton, Alberta T6G 2G1 Canada
E-mail address: `ylin@hilbert.math.ualberta.ca`